Picosecond infrared optical parametric amplifier for nonlinear interface spectroscopy

D. Bodlaki and E. Borguet[a)]
Department of Chemistry and Surface Science Center, University of Pittsburgh, 219 Parkman Avenue, Pittsburgh, Pennsylvania 15260

(Received 27 June 2000; accepted for publication 3 September 2000)

A tunable, narrow bandwidth, high peak power picosecond infrared (IR) laser system is described. The pump source is a picosecond Ti:sapphire regenerative amplifier seeded by a picosecond Ti:sapphire oscillator. The pump bandwidth and pulse duration are tunable producing 4–5 ps, 5–4 cm^{-1} pulses at 1 kHz. IR pulses are produced by optical parametric generation (OPG) followed by optical parametric amplification (OPA). Tuning is possible over the entire 1050–3300 nm region of the IR, with energies in excess of 15 μJ over most of the range. The temporal and spectral characteristics of the IR pulses are reviewed with a particular focus on the sources of bandwidth broadening in the OPG/OPA. Bandwidth optimization of the IR output is discussed. A spectral filtering scheme results in less than 15 cm^{-1} IR bandwidth, suitable for nonlinear optical spectroscopic applications. © *2000 American Institute of Physics.* [S0034-6748(00)02012-8]

I. INTRODUCTION

The investigation of fundamental chemical and physical dynamical processes requires optical sources that optimize spectral and temporal resolution. This is particularly important for nonlinear optical spectroscopies such as second harmonic generation (SHG) and sum frequency generation (SFG) that are highly interface specific.[1–4] Spectroscopic SHG and SFG require wavelength tunable sources providing high peak powers. Narrow bandwidth $\Delta\tilde{\nu}$ is required to resolve closely spaced spectral features. Short pulses τ are required to probe fast dynamics and to provide peak powers for efficient SHG/SFG. The Fourier transform limit $\Delta\tilde{\nu}\tau$ determines the optimal achievable compromise. A 100 fs Gaussian pulse, for example, has a 150 cm^{-1} transform limited bandwidth. This is an order of magnitude greater than the bandwidth desirable for condensed phase vibrational spectroscopy.

We report a 1 kHz, picosecond optical parametric amplifier (OPA), pumped by a picosecond Ti:sapphire regenerative amplifier, providing tunable infrared (IR) in the 1000–3500 nm range with less than 15 cm^{-1} bandwidth. This device has the necessary spectral and temporal resolution to address many interface issues. The OPA design offers the potential to tailor the source temporal and spectral characteristics for each experiment.

It is useful to review the different sources used for surface nonlinear spectroscopy. These fall into three broad categories, ns-long ps, short ps-fs, and free electron lasers. The earliest surface IR+visible (VIS) SFG experiments used a fixed wavelength ns visible (532 nm of Nd:YAG) and a tunable ns IR laser (CO_2).[5] Soon thereafter OPAs were employed for SFG.[6] In various forms, OPAs have been the workhorse for IR generation for SFG experiments, though difference frequency generation in nonlinear crystals[7] and Raman shifting [8,9] have also been used to produce tunable IR for SFG.

Free electron lasers offer a number of attractive features for IR+VIS SFG, not the least of which are their broad tunability in the IR (1–100 μm) and high pulse energy (>20 μJ).[10,11] However, the requirement to travel to a dedicated facility has limited their use to a few groups.

The generation of spectrally narrow pulses requires long temporal pulses. Nanosecond OPO/OPA approaches have been used successfully by a number of groups.[12] However, if temporal resolution and signal levels are not to be sacrificed, shorter pulses are required. Pulses that are a few picoseconds long with bandwidth <20 cm^{-1} provide the spectral and temporal resolution, as well as the necessary signal levels appropriate for most interface science questions.

Transform limited Gaussian 3 ps pulse generation has been achieved by the Laubereau group.[13] This requires the use of a Nd:yttrium–lithium–fluoride (Nd:YLF) synchronously pumped optical parametric oscillator as the seed source for the OPA.[14] A common drawback of Nd:yttrium–aluminum–garnet (Nd:YAG) systems is their low repetition rate, typically 10 Hz. This reduces the signal generated per second, an important consideration when the photon counting statistics dominate the signal to noise ratio.

The development of femtosecond kHz Ti:sapphire regenerative amplifiers in the early 1990s has led to an explosion in tunable IR and VIS optical parametric sources.[15–19] These are typically based on a broadband, continuum generation seeding stage.[15,18] Continuum generation is a very effective process in the 10^{-13} s regime, requiring <1 μJ and producing little sample damage. Spectroscopic SFG spectra have been obtained by mixing the broadband femtosecond IR with a spectrally narrowed visible pulse for IR+VIS SFG.[20] Recently, the Shen group showed that interferometric SFG with broadband fs IR pulses can yield high resolution (<7 cm^{-1}) interface spectra.[21] A potential disadvantage of

a)Author to whom correspondence should be addressed; electronic mail: borguet+@pitt.edu

approaches that employ broadband (>50 cm^{-1}) IR is that the output can excite multiple distinct oscillators simultaneously. However, this inconvenience can be turned into an advantage; ultrashort broadband IR pulses are ideal for quantum beat SFG spectroscopy.[22]

The Richmond group at the University of Oregon recently took advantage of the availability of picosecond kHz Ti:sapphire regenerative amplifiers to produce narrow bandwidth tunable IR.[23,24] There are several notable differences between the Oregon system and the one reported here. The Oregon pump is a 2 ps, 17 cm^{-1} source [>2 times transform limit (TL) of a Gaussian pulse], while the present pump provides a 4–5 ps pulse, 5–4 cm^{-1} (1.4×TL). As the pump spectral width ultimately limits the bandwidth of the OPA output, a 5 cm^{-1} pump offers the potential for spectrally narrower IR pulse generation than a 17 cm^{-1} source. The Oregon seed is provided by a continuum, whereas the OPA discussed here used parametric fluorescence. Continuum generation in the ps domain is unstable, easily damaging the medium in which it is performed and requires >100 μJ, more than two orders of magnitude the energy that is required in femtosecond OPAs. This consumes energy that could otherwise be employed for experiments.

II. THEORETICAL CONSIDERATIONS

A number of nonlinear crystals are available for infrared generation. We have chosen KTP because it possesses a high damage threshold (80 GW/cm^2 reported for 2 ps, 1 kHz 800 nm pumping),[23] high nonlinearity, and wide transparency range (0.35–4 μm). The performance of a crystal depends on its effective nonlinearity, d_{eff}. Although KTP is a biaxial crystal, it can be treated as a uniaxial crystal because the refractive index n_z (1.8297 at 1 μm) is larger than n_x (1.7377) and n_y (1.7453), and n_x and n_y differ slightly.[25] The effective nonlinear coefficient d_{eff} can be approximated by

for type I phase matching

$$d_{\text{eff}} \approx 1/2(d_{15}-d_{24})\sin 2\theta \sin 2\phi, \tag{1}$$

for type II phase matching

$$d_{\text{eff}} \approx (d_{24}-d_{15})\sin 2\theta \sin 2\phi - (d_{15}\sin^2\phi + d_{24}\cos^2 2\phi)\sin\theta, \tag{2}$$

where θ is the angle the propagation direction makes with the z axis and ϕ is the angle in the xy plane of the crystal.[25] For KTP the nonlinear coefficients are $d_{15}\sim 2.04$ pm/V, $d_{24}\sim 3.92$ pm/V at 880 nm, close to our pump wavelength, 800 nm.[26] Equations (1) and (2) suggest that type II phase matching offers higher nonlinearity than type I phase matching. We have considered three cases of type II phase matching in KTP crystal: phase matching in xz, xy, and yz planes. Phase matching in xz and yz planes provides the widest tuning range (1–4 μm). Type II phase matching in the xz plane has the highest d_{eff}.[27]

Two polarization schemes are possible when phase matching in the xz plane. Ordinary idler and extraordinary signal are generated for $\theta<52°$. The opposite combination of signal and idler waves can be generated for $\theta>52°$ (Fig. 1) with a higher nonlinearity but a reduced tuning range.

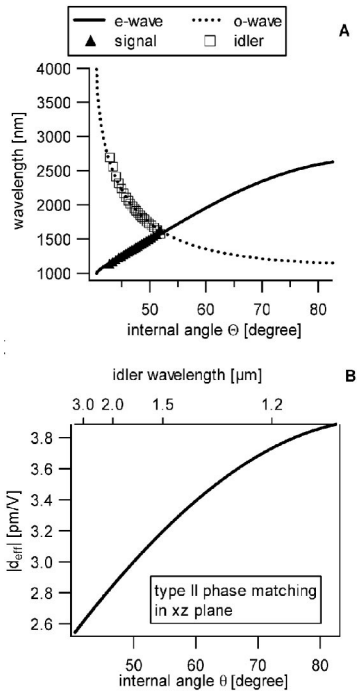

FIG. 1. Theoretical and experimental tuning curve (A) and theoretical values of effective nonlinearity d_{eff} (B) for type II phase matching in the KTP xz plane. On the phase matching curve (A), the circles are measured signal (e) wavelength and squares are measured idler (o) wavelength. The o wave denotes ordinary wave, e wave denotes extraordinary wave. The line is the calculated phase matching angles.

Taking account of all these factors, type II phase matching in the xz plane was selected, with $\theta<52°$ so that an ordinary pump generates an extraordinary signal and an ordinary idler.

III. EXPERIMENT

A. Characterization tools

The Ti:sapphire oscillator, regenerative amplifier, and OPA were characterized in terms of output power, wavelength, bandwidth, and pulse duration. The wavelength of OPA was measured by SHG, in single crystal quartz, sent to a monochromator (Acton Research, SP-300i, 300 groove/mm (gr/mm) grating, blazed at 1 μm, 11 nm/mm dispersion), and detected by a liquid nitrogen-cooled charge coupled device (CCD) (Princeton Instrument CCD30-11, 26×26 μm pixel size, 0.3 nm/pixel resolution). The bandwidth [full width at half maximum (FWHM)] of the oscillator and regenerative amplifier output was measured using the 1800 gr/mm grating (optimized for 0.35–1.1 μm) in the monochromator and CCD (0.03 nm/pixel resolution). The signal and idler bandwidths were measured using the 300 gr/mm monochromator grating (resolution is 2 nm at 1 μm) and infrared InSb (1–5 μm) or InGaAs (0.8–1.8 μm, Thorlabs) detectors. Power was measured by a power meter (Thorlabs). The oscillator and regenerative amplifier pulse width were determined by autocorrelation. The signal and idler pulse width was measured by crosscorrelation of the infrared pulses with 800 nm pulses in a 2 mm thick BBO. Autocorrelation and crosscorrelation signals were detected

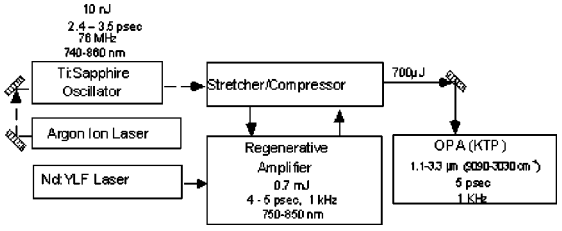

FIG. 2. Diagram of the Ti:sapphire regenerative amplifier and optical parametric amplifier. The Ti:sapphire oscillator pumped by an Ar ion laser provides 2.4–3.5 ps pulses with 10 nJ/pulse energy at 76 MHz repetition rate tunable 740–860 nm. Regenerative amplifier pumped by a Nd:YLF laser amplifies pulses to 0.7 mJ/pulse energy at 1 kHz repetition rate. The output of the amplifier is sent to the optical parametric amplifier for frequency conversion to the infrared.

by a Si photodiode (Thorlabs), connected to a boxcar interfaced with a computer. Beam diameters were determined by knife-edge measurement.[28]

B. Ti:sapphire laser system

The seed pulses for the Ti:sapphire system are supplied by a picosecond Ti:sapphire oscillator (Coherent Mira 900 F/P) pumped by all lines (485, 514.5, . . . nm) of an Ar^+ ion laser (Coherent Innova 310C) (Fig. 2). The Ti:sapphire oscillator provides a 2.4–3.5 ps, 76 MHz pulse train, with >10 nJ/pulse energy, tunable in the 750–850 nm wavelength range. While the output of the oscillator is adequate for many nonlinear optical experiments, the pulse energy is too low for significant population transfer to excited states and the repetition rate is too high for some systems to recover to their initial state between successive pulses. What is needed is an increase of pulse energy and increase of the time between pulses. Both of these are achieved in the regenerative amplifier. A single temporally stretched seed pulse is selected by a Pockels cell (Medox) and further amplified in Ti:sapphire regenerative amplifier (Alpha-1000, BMI-Coherent) pumped by the second harmonic (527 nm) of a Nd:YLF (BMI-Coherent). To avoid optical damage in the regenerative amplifier so called chirped pulse amplification is applied to reduce the high peak power densities that would otherwise by present due to short (1–4 ps) pulse durations.[29] Pulses are stretched before amplification to pulse durations >100 ps. Subsequent compression after amplification returns the pulse duration to close to the initial preamplifiction values. Security systems monitor the pulse parameters (repetition rate and bandwidth) before the pulse enters the stretcher and aborts the amplifier operation when the seed has the potential (loss of mode locking, . . .) to damage the optics in the amplifier. After compression the regenerative amplifier output is centered around 800 nm, providing 4–5 ps pulses with >700 μJ energy and 1 kHz repetition rate.

The oscillator and regenerative amplifier pulses were temporally and spectrally characterized. Figure 3(A) shows the autocorrelation trace of the Ti:sapphire oscillator pulse. It is well described by a Gaussian pulse shape with 3.5 ps FWHM, corresponding to a 2.5 ps pulse duration. The time–bandwidth product sets a limit to the smallest possible bandwidth that can be achieved for a given pulse duration. For a Gaussian pulse the time–bandwidth product is 0.441, giving

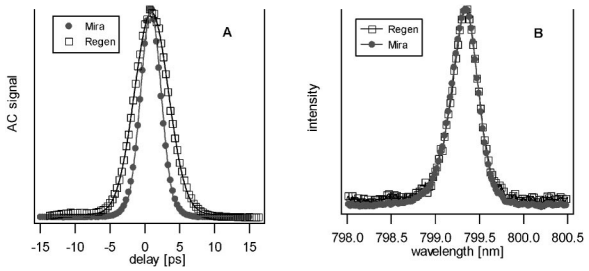

FIG. 3. Autocorrelation (A) and spectrum (B) of the Ti:sapphire oscillator (solid circles) and the regenerative amplifier (open squares). In the pulse width measurement (A), the solid line is a Gaussian fit, FWHM is 3.5 ps for the oscillator, and 5.8 ps for the amplifier. The corresponding pulse duration is 2.7 ps for the oscillator and 4.1 ps for the amplifier. In the bandwidth measurement (B), the solid line is a guide to the eye. The oscillator bandwidth is 0.37 nm, and the amplifier bandwidth is 0.37 nm.

0.35 nm as the transform limited bandwidth at 800 nm. The bandwidth of the oscillator was measured to be 0.37 nm [Fig. 3(B)] indicating that the oscillator output is 1.1 times transform limited. For comparison, the autocorrelation trace and spectrum of the amplified pulse are also shown in Fig. 3. The amplified pulse is also described well by a Gaussian with 5.8 ps FWHM, corresponding to a pulse duration of 4.1 ps. The bandwidth was measured to be 0.37 nm. This indicates 1.6 times transform limited amplifier pulses. While the amplifier pulse does not appear to have been perfectly recompressed, stretching and compression do not strongly modify the spectral parameters of the pulse.

The pulse duration of the Ti:sapphire oscillator seed can be varied in the 2.4–3.5 ps range. Bandwidth changes accordingly from 0.37 to 0.27 nm. The output of the regenerative amplifier follows the pulse width and bandwidth changes of oscillator seed. The pulse width changes from 3.8 to 4.9 ps, with accompanying bandwidth changes from 0.37 to 0.27 nm.

C. Optical layout of OPA

The OPA design adopted is based on a first stage of parametric generation followed by several stages of amplification. Figure 4 shows the OPA optical layout. The output of the regenerative amplifier is split into two pump arms to pump two OPA stages. The first stage consists of a single KTP crystal (KTP1) in a double pass geometry. The second

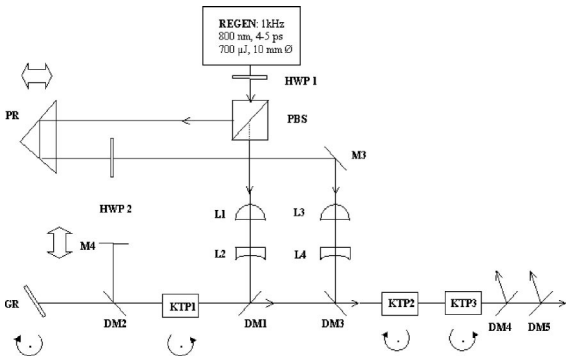

FIG. 4. Layout of the optical parametric amplifier: (HWP) half-wave plate, (PBS) polarizing beamsplitter, (*L*) lens, (*M*) silver mirrors, (DM) dichroic mirrors, (KTP) nonlinear crystals, (GR) grating, (PR) prism.

stage consists of one or two crystals (KTP2 and KTP3) employed in single pass configuration. All KTP crystals are $5\times6\times10$ mm and cut at $\theta=47.2°$, $\phi=0°$. The combination of a half wave plate (HWP1) and polarizing beam splitter enables the power in each arm to be varied.

The first stage pump is horizontally polarized. It passes through a telescope that reduces the beam diameter by 10:1. The pump beam is directed to KTP1 by a dichroic mirror (DM1). The dichroic mirrors (DM1–DM4) reflect 800 nm ($R_{800}>99.5\%$) and transmit 1–4.2 μm ($T_{\text{ave}}>95\%$). The beam diameter of the pump at KTP1 is 600 μm (340 mW average power, peak power density 28 GW/cm^2). In the first pass, IR photons at signal and idler wavelengths are generated by optical parametric generation (OPG) in KTP1. The generated IR passes through DM2 which transmits IR and reflects 800 nm. The signal wavelength is sent back to KTP1 for amplification after diffraction off the grating (GR) (600 gr/mm, blazed at 1 μm or 1200 gr/mm grating blazed at 1 μm). The 800 nm pump light is reflected back from a silver mirror (*M*4) and combined with signal seed at DM2. *M*4 is placed on a translation stage so that the signal and pump pulses can be temporally overlapped (delay 1). In the second pass in KTP1, amplification of signal wavelength and generation of idler wavelength occur. The pump beam diameter on the second pass at KTP1 is 1 mm (300 mW average power, 9 GW/cm^2). The signal beam diameter is 200 μm. After the first stage, combined signal and idler energies as high as 4 μJ/pulse are achieved. The amplification factor in the second pass was determined to be 10^5.

About 260 mW of pump is directed to the second stage of the OPA through a delay line (delay 2). It is horizontally polarized after the HWP2 and passes through a 7:1 reduction ratio telescope. The 800 nm pump is combined with IR from the first stage (KTP1). The beam diameter of the pump is 580 μm (23 GW/cm^2) at KTP2. The diameter of the IR beam is 260 μm at KTP2. Currently, both signal and idler are used to seed the second stage of the OPA. In general, seeding with only one wavelength creates a simpler, more controllable situation. Seeding with the idler has been reported to result in higher idler energies and qualitatively better beam profile.[23]

The second stage can accommodate one or two KTP crystals. When two KTP crystal are used, they are placed in such a way that when angle tuning the OPA they rotate in opposite directions. In this way, beam displacement caused by the rotation of one crystal can be compensated by an equal amount of rotation of the other crystal. KTP3 also provides additional amplification as shown in Fig. 5.

After passing through KTP2 and KTP3, the 800 nm light is separated from the IR by a dichroic mirror (DM4). Further filtering of the OPA output depends on the application.

The wavelength tuning of the OPA is achieved by rotation of the KTP crystals and the GR. The crystals and grating are placed on rotating stages which are driven by stepper motors (0.03 mrad/step). During wavelength scanning a computer program (LABVIEW) controls the rotation stages and data collection.

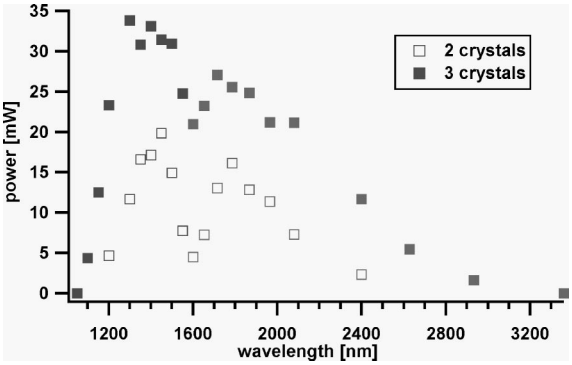

FIG. 5. Signal ($\lambda<1600$ nm) and idler ($\lambda>1600$ nm) power as a function of wavelength. Open squares were measured with a two-crystal configuration, filled squares with a three-crystal configuration.

IV. RESULTS AND DISCUSSION

A. Tuning behavior

The wavelength range and output power over this wavelength range are primarily determined by the properties of the nonlinear crystal. The phase matching angles are determined from the wavelength dependence of the refractive indices, given by the Sellmeier equations.[25] The theoretical and measured phase matching curve providing the wavelength produced versus orientation of the crystal, are shown in Fig. 1. The measured data reproduces well the predicted phase matching angles calculated using published refractive indices.[27]

The signal and idler output power as a function of wavelength is shown in Fig. 5. During the measurement no intermediate alignment of the OPA was made. The initial configuration contained two KTP crystals. The tuning range was limited to the 1.2–2.4 μm range, although KTP should enable the generation of wavelengths as long as 4 μm.[23]

Similar tuning behavior was reported by Carrion and Girardeau-Montaut and was attributed to a decrease of effective nonlinearity d_{eff} as idler wavelength increased.[30] The calculated dependence of d_{eff} on wavelength is depicted in Fig. 1. To estimate the effect of the wavelength dependence of d_{eff}, the amplification in a single pass was calculated considering a 10 mm long KTP and 25 GW/cm^2 (power density at KTP2) pump pulse. In the strong gain regime, the amplification A is exponential in gain Γ over the interaction length L:

$$A=1/4e^{2L\Gamma}. \tag{3}$$

The gain is principally determined by the effective nonlinearity d_{eff} when perfect phase matching ($\Delta k=0$) is assumed:

$$\Gamma_0=\left(\frac{8\pi^2 I_p\tilde{\nu}_s\tilde{\nu}_i}{c\epsilon_0 n_i n_s n_p}\right)^{1/2} d_{\text{eff}}, \tag{4}$$

where I_p is the pump peak power density, $\tilde{\nu}_s$ and $\tilde{\nu}_i$ are the wave number of signal and idler, n_p, n_s, n_i are the refractive indices of pump, signal, and idler, respectively, and d_{eff} is the effective nonlinear coefficient.[27,31] Under these conditions, amplification varies by 6 orders of magnitude over the entire tuning range of KTP (1–4 μm) (Fig. 6). Equations (3) and (4) depict an ideal situation where losses due to im-

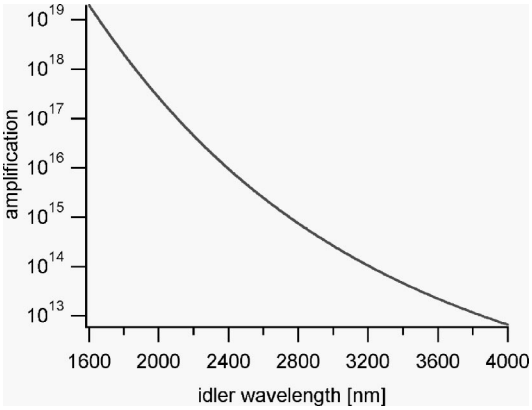

FIG. 6. Estimated amplification for KTP type II phasematching in the *xz* plane. Calculation is based on Eqs. (3) and (4) taking pump power 25 GW/cm^2, crystal length 1 cm.

proper spatial and temporal overlap (walkoff and group velocity mismatch effects) are not considered. The experimentally observed behavior (Fig. 5) suggests that the OPA is operating in the saturated regime. Such behavior has been observed previously by others.[27]

Other possible factors that limit the tuning range were considered. These include transmission of dichroic mirrors (DM1–DM4), loss of 800 nm pump due to reflection from the crystal surface, and efficiency of diffraction in first order from the grating. These factors were carefully investigated and optical elements were chosen so that these losses are minimized. In addition, it is not expected that such factors would show the strong wavelength dependence depicted in Fig. 5.

Equation (3) shows that the longer the interaction length L, the more amplification is achieved. Our conclusion is that the limited wavelength range is due to insufficient amplification. This suggests that in order to achieve wider wavelength tuning range, three or four KTP crystals would be necessary. We added a third crystal to test this hypothesis. The OPA efficiency improved and the tuning range expanded by more than 200 nm to longer idler wavelengths (Fig. 5).

B. Bandwidth measurement

To resolve spectroscopic features a narrow-bandwidth source is necessary. For instance, the vibrational spectra of air/octadecyltrichlorosilane/glass interface shows modes typically about 10 cm^{-1} wide and separated by 10–100 cm^{-1} from each other.[32] Sources with bandwidth larger than 10 cm^{-1} would broaden features and might not resolve separate modes. Even broader pulses, such as provided by fs lasers, would excite several oscillators simultaneously.

The spectral bandwidth of the OPA output is determined by several factors, including the gain bandwidth, the pump divergence, and the divergence of the generated signal and idler beams.[31,33] When phase matching is not perfect ($\Delta k \neq 0$), the gain is reduced. The FWHM of the gain curve (gain versus Δk) is called the gain bandwidth ($\Delta k_{1/2}$). It was estimated to be about 46 cm^{-1} at idler wavelength $\lambda_i = 1920$ nm using Eq. (5):

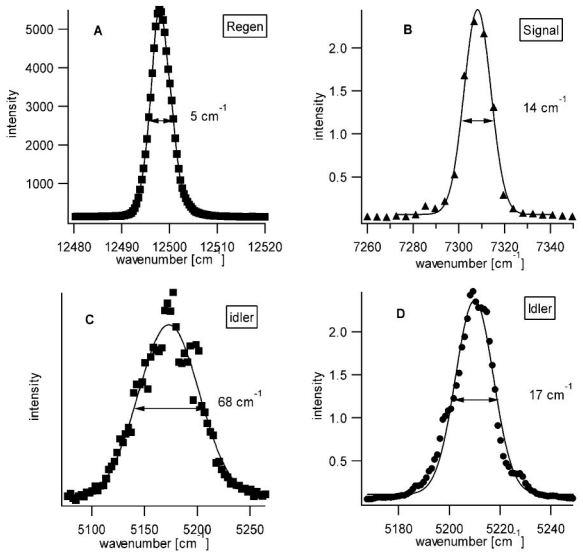

FIG. 7. Bandwidth of pump and signal, idler wavelength: (A) spectra of pump. Bandwidth of pump is 5 cm^{-1}, (C) bandwidth of idler when there is no grating in OPA. In this condition idler bandwidth is 68 cm^{-1}. For comparison, (B) and (D) show signal and idler bandwidth with 1200 gr/mm (blazed at 1 μm) grating in OPA. Signal and idler bandwidths are 14 and 17 cm^{-1}, respectively.

$$\Delta k_{1/2} = \frac{1}{L}((2\ln 2)(2\Gamma_0 L))^{1/2}, \tag{5}$$

where L is the interaction length and Γ_0 is defined by Eq. (4).[33] The pump beam divergence contributes to the bandwidth as follows. The finite divergence ϕ of the pump means that the phase matching angle varies spatially across the pump diameter. As a result, a range of signal-idler wavelengths is generated. The pump beam divergence was measured to be $\sim$1 mrad, giving rise to 8 cm^{-1} bandwidth contribution. The generated signal beam also has a finite divergence. This enables noncollinear phase matching, generating wavelengths different from those of collinear phase matching. The signal divergence can be approximated by $\alpha = d/L$, where d is the pump beam diameter and L is the crystal length.[31] Considering a 580 μm pump beam diameter (at KTP2) and $L = 1$ cm crystal, a bandwidth contribution of 33 cm^{-1} is calculated.

Taking into account all these contributions (gain bandwidth, pump divergence, and divergence of signal beam), the overall bandwidth is determined to be $\delta\tilde{\nu} \approx (\delta\tilde{\nu}_1^2 + \delta\tilde{\nu}_2^2 + \delta\tilde{\nu}_3^2)^{1/2} = (46^2 + 8^2 + 33^2)^{1/2} = 62$ cm^{-1} at idler wavelength $\lambda_i = 1920$ nm. The idler bandwidth before any attempt to narrow the bandwidth is 68 cm^{-1} (Fig. 7). This is consistent with our estimates.

There are a number of ways to control the bandwidth. Lowering the pump power reduces the gain bandwidth. A proper choice and adjustment of the telescopes can reduce the pump divergence and the pump beam diameter. Another means to control the bandwidth is the use of a bandwidth narrowing element, such as a grating, between the OPG and amplification stages.

The infrared output generated in the first pass through KTP1 was sent to a grating to narrow the seed bandwidth. The signal wavelength was diffracted off the grating and

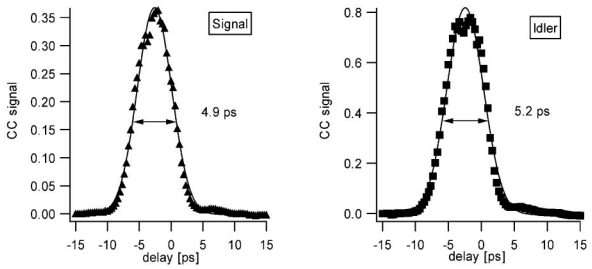

FIG. 8. Crosscorrelation of signal and idler pulses. Solid line is Gaussian fit. FWHMs are 6.4 and 6.8 ps; corresponding pulse duration are 4.9 and 5.2 ps for signal and idler pulses, respectively.

directed back to KTP1. The grating was placed in Littrow geometry where the first order diffraction is sent back in the direction of the incident beam. The Littrow geometry was favored over Litmann–Metcalf geometry[34] because of the ease of alignment but also because grating performance was optimized for this geometry. Gratings with groove density of 600 gr/mm (blazed at 1 μm) and 1200 gr/mm (blazed at 1 μm) were tested. The bandwidth falling within the overlapping area of the pump and the diffracted signal at KTP1 can be estimated from the grating equation

$$\delta\tilde{\nu} \approx \tilde{\nu}^2 a \frac{d}{D} \cos\alpha, \tag{6}$$

where a is the groove spacing, d is the beam diameter of the IR beam, D is the distance between the grating and the KTP crystal and α is the angel of incidence on grating. At a signal wavelength of 1370 nm, Eq. (6) shows that a bandwidth of 9.1 cm^{-1} (600 gr/mm) or 2.8 cm^{-1} (1200 gr/mm) is achievable with these gratings. The pump bandwidth, 5 cm^{-1} (Fig. 7) limits the best achievable bandwidth in the latter case. The measured signal bandwidth is reduced from 45 to 19.5 cm^{-1} when a 600 gr/mm grating is used in OPA (not shown). The 1200 gr/mm grating further reduces the measured signal bandwidth to 14 cm^{-1}as shown in Fig. 8(B). The idler bandwidth with the same grating is 17 cm^{-1} [Fig. 7(D)]. This is approximately three times broader than the pump bandwidth. The signal/idler bandwidth is not limited by the grating or the pump bandwidth. The preceding analysis suggests that further improvement can be made by controlling the pump beam diameter and divergence. This should be achievable without sacrificing the power performance of OPA.

C. Pulse width measurement

The pulse duration of the output signal and idler were determined. The signal and idler pulse widths were measured by crosscorrelation of the signal and idler with 800 nm in a 2 mm BBO crystal. Figure 8 shows the crosscorrelation of the signal and idler pulses. The Regen pulse width, assuming a Gaussian pulse shape, is 4.1 ps (Fig. 3). The signal and idler pulse width were extracted by assuming convolution of two Gaussians ($dt_{cc}^2 = dt_p^2 + dt_i^2$). A crosscorrelation FWHM of 6.4 ps (6.6 ps) was obtained for the signal (idler), resulting in 4.9 ps (5.2 ps) pulsewidth. The signal and idler pulses are about 1.3 times longer than the pump pulse.

Assuming Gaussian pulse shapes for the Regen and OPA output, the Regen input pulse is 1.4 times transform limited, while the signal pulse is five times transform limited for 1200 gr/mm grating.

D. Future directions

The three-crystal configuration provides sufficient power for spectroscopic and dynamic studies. However, intermediate alignment of the amplifier might improve efficiency in ranges farther from the normal incidence position of the crystals ($\lambda_{idler} \approx 1920$ nm), where the OPA is optimized before tuning. As discussed, the bandwidth can be further narrowed by control of pump beam diameter and focusing.

The quality of the input beams is important in nonlinear optical processes.[24] Strong focusing of the pump beam in the OPA crystals results in elliptical beam shapes and reduces the efficiency of second harmonic generation. In the current second stage configuration, the distance between the two crystals (KTP2 and KTP3) is fixed. An adjustable distance between the crystals would give more control of focusing on the individual crystals and consequently ore control over the output beam quality. Beam diameter could be better matched with other telescope reduction ratios.

In conclusion, an automated picosecond infrared optical parametric amplifier tunable in the 1.1–3.3 μm range with approximately 15 cm^{-1} bandwidth has been reported for the purpose of combined spectroscopic and dynamic studies. The OPA is based on three KTP crystals, all type II phase matched in the xz plane. A grating is used to minimize the output bandwidth to about 15 cm^{-1} making the OPA suitable for spectroscopic studies. Without a grating, a bandwidth >60 cm^{-1} was measured. Wavelength tuning of the OPA is achieved by automated angle tuning of the nonlinear crystals and the grating. The pulse width of the output was measured to be close to the pump pulse width, indicating that the parametric process does not effect pulse width significantly in this design.

ACKNOWLEDGMENTS

The authors would like to thank two REU students, Andy Vidan and An Ngo, for their contributions. The REU program is supported by NSF Grant No. PHY95-31628. This work was supported by NSF Grant No. CHE-9734273.

[1] Y. R. Shen, *The Principles of Nonlinear Optics* (Wiley, New York, 1984).
[2] R. M. Corn and D. A. Higgins, Chem. Rev. **94**, 107 (1994).
[3] K. B. Eisenthal, Chem. Rev. **96**, 1343 (1996).
[4] G. L. Richmond, Anal. Chem. **69**, 536A (1997).
[5] X. D. Zhu, H. Suhr, and Y. R. Shen, Phys. Rev. B **35**, 3047 (1987).
[6] X. D. Hunt, P. Guyot-Sionnest, and Y. R. Shen, Chem. Phys. Lett. **133**, 189 (1987).
[7] D. Zhang, J. H. Gutow, K. B. Eisenthal, and T. F. Heinz, J. Chem. Phys. **98**, 5099 (1993).
[8] A. L. Harris, C. E. D. Chidsey, N. J. Levinos, and D. N. Loiacono, Chem. Phys. Lett. **141**, 350 (1987).
[9] G. R. Bell, S. ManningBenson, and C. D. Bain, J. Phys. Chem. B **102**, 218 (1998).
[10] A. Peremans, A. Tadjeddine, P. Guyot-Sionnest, R. Prazeres, F. Glotin, D. Jaroszynski, J. M. Berset, and J. M. Ortega, Nucl. Instrum. Methods Phys. Res. A **341**, 146 (1994).
[11] M. Barmentlo, G. W. Thooft, E. R. Eliel, E. W. M. Vanderham, Q. H. F. Vrehen, A. F. G. Vandermeer, and P. W. Vanamersfoort, Phys. Rev. A **50**, R14 (1994).

[12] R. A. Walker, B. L. Smiley, and G. L. Richmond, Spectroscopy (Amsterdam) **14**, 18 (1999).
[13] K. Wolfrum, J. Lobau, and A. Laubereau, Appl. Phys. A: Mater. Sci. Process. **59**, 605 (1994).
[14] K. Wolfrum, H. Graener, and A. Laubereau, Chem. Phys. Lett. **213**, 41 (1993).
[15] V. V. Yakovlev, B. Kohler, and K. R. Wilson, Opt. Lett. **19**, 2000 (1994).
[16] P. E. Powers, R. J. Ellingson, W. S. Pelouch, and C. L. Tang, J. Opt. Soc. Am. B **10**, 2162 (1993).
[17] V. Petrov and F. Noack, J. Opt. Soc. Am. B **12**, 2214 (1995).
[18] S. R. Greenfield and M. R. Wasielewski, Opt. Lett. **20**, 1394 (1995).
[19] B. Akhremitchev, C. F. Wang, and G. C. Walker, Rev. Sci. Instrum. **67**, 3799 (1996).
[20] L. T. Richter, T. P. Petralli Mallow, and J. C. Stephenson, Opt. Lett. **23**, 1594 (1998).
[21] J. A. McGuire, W. Beck, X. Wei, and Y. R. Shen, Opt. Lett. **24**, 1877 (1999).
[22] D. Star, T. Kikteva, and G. W. Leach, J. Chem. Phys. **111**, 14 (1999).
[23] D. E. Gragson, D. S. Alavi, and G. L. Richmond, Opt. Lett. **20**, 1991 (1995).
[24] D. E. Gragson, B. M. McCarty, and G. L. Richmond, J. Opt. Soc. Am. B **13**, 2075 (1996).
[25] R. W. Munn and C. N. Ironside, *Principles and Applications of Nonlinear Optical Materials* (Blackie Academic & Professional, London, 1993).
[26] H. Vanherzeele and J. D. Bierlein, Opt. Lett. **17**, 982 (1992).
[27] J. D. Bierlein and H. Vanherzeele, J. Opt. Soc. Am. B **6**, 622 (1989).
[28] A. E. Siegman, in *Solid State Lasers: New Developments and Applications*, edited by M. Inguscio and R. Wallenstein (Plenum, New York, 1993), p. 13.
[29] P. Strickland and G. Mourov, Opt. Commun. **56**, 219 (1985).
[30] L. Carrion and J. P. Girardeau-Montaut, Opt. Commun. **152**, 347 (1998).
[31] A. Seilmeier, K. Spanner, A. Laubereau, and W. Kaiser, Opt. Commun. **24**, 237 (1978).
[32] P. Guyot-Sionnest, R. Superfine, J. H. Hunt, and Y. R. Shen, Chem. Phys. Lett. **144**, 1 (1988).
[33] J. Y. Zhang, J. Y. Huang, Y. R. Shen, and C. Chen, J. Opt. Soc. Am. B **10**, 1758 (1993).
[34] M. G. Littman and H. J. Metcalf, Appl. Opt. **17**, 2224 (1978).